

First Constraint on P-odd/T-odd Cross Section in Polarized Neutron Transmission through Transversely Polarized ^{139}La

Rintaro Nakabe¹, Clayton J. Auton², Shunsuke Endo¹, Hiroyuki Fujioka³,
 Vladimir Gudkov⁴, Katsuya Hirota⁵, Ikuo Ide⁶, Takashi Ino⁵,
 Motoyuki Ishikado⁷, Wataru Kambara¹, Shiori Kawamura^{6,1},
 Atsushi Kimura¹, Masaaki Kitaguchi⁶, Ryuju Kobayashi¹,
 Takahiro Okamura⁵, Takayuki Oku^{1,8}, Takuya Okudaira^{6,1}, Mao Okuizumi⁶,
 J. G. Otero Munoz², Joseph D. Parker⁷, Kenji Sakai¹, Tatsushi Shima⁹,
 Hirohiko M. Shimizu⁶, Takenao Shinohara¹, William M. Snow²,
 Shusuke Takada^{10,1}, Ryuta Takahashi¹, Shingo Takahashi¹¹,
 Yusuke Tsuchikawa¹, and Tamaki Yoshioka¹²

¹*Japan Atomic Energy Agency, 2-4 Shirakata, Tokai, Ibaraki 319-1195, Japan*

**E-mail: nakabe.rintaro@jaea.go.jp*

²*Indiana University, Bloomington, Indiana 47401, USA*

³*Institute of Science Tokyo, Meguro, Tokyo 152-8551, Japan*

⁴*University of South Carolina, Columbia, South Carolina 29208, USA*

⁵*High Energy Accelerator Research Organization, 1-1 Oho, Tsukuba, Ibaraki 305-0801, Japan*

⁶*Nagoya University, Furocho, Chikusa, Nagoya 464-8602, Japan*

⁷*Comprehensive Research Organization for Science and Society, Tokai, Ibaraki 319-1106, Japan*

⁸*Ibaraki University, 2-1-1 Bunkyo, Mito, Ibaraki 310-8512, Japan*

⁹*Osaka University, Ibaraki, Osaka 567-0047, Japan*

¹⁰*Tohoku University, 2-1-1 Katahira, Aoba, Sendai, 980-8576 Japan*

¹¹*The University of Tokyo, Kashiwa, Chiba 277-8581, Japan*

¹²*Kyushu University, 744 Motoooka, Nishi, Fukuoka 819-0395, Japan*

.....
We report the first constraint on time-reversal invariance violating (TRIV) effects in polarized neutron transmission through a polarized ^{139}La target. Using the explicit forward scattering amplitude for ^{139}La , we derive analytic expressions for spin observables within the density matrix formalism and apply them to the existing transmission data. The experiment was not optimized for TRIV observables but was taken to measure the spin-dependent cross section around the p -wave resonance, which intrinsically limits the attainable sensitivity. To extract a robust TRIV constraint under these conditions, we performed a χ^2 fit treating p -wave resonance energy E_p as a Gaussian-constrained nuisance parameter. The fit showed no evidence for TRIV effects. We set an upper limit on the TRIV cross section of $|\Delta\sigma_{TP}| < 1.2 \times 10^2$ b averaged over the resonance region. These results validate the theoretical approach and demonstrate the feasibility of future dedicated TRIV searches using a polarized neutron beam and a polarized nuclear target.
.....

Subject Index D00, D21, C03

1 Introduction

The search for time-reversal invariance violating (TRIV) effects offers an experimental approach to exotic CP-violations beyond the standard model of elementary particles via the CPT theorem. A novel experimental possibility to search for TRIV effects in behavior of neutron spin propagating in polarized nuclear targets is under study by the collaboration of “Neutron Optical and Time-Reversal Experiment” (NOPTREX) partially as the J-PARC E99. A sensitive probe of TRIV effects is provided by measuring the transmission of low-energy polarized neutrons through a polarized nuclear target [1–3]. The forward elastic scattering amplitude for such neutrons can be expressed as the sum of a spin-independent term and three spin-dependent terms:

$$f = \alpha + \boldsymbol{\beta} \cdot \boldsymbol{\sigma}_n, \quad \boldsymbol{\beta} = \beta_{\hat{\mathbf{I}}} \hat{\mathbf{I}} + \beta_{\hat{\mathbf{k}}_n} \hat{\mathbf{k}}_n + \beta_{\hat{\mathbf{k}}_n \times \hat{\mathbf{I}}} \hat{\mathbf{k}}_n \times \hat{\mathbf{I}} \quad (1)$$

where $\boldsymbol{\sigma}_n = (\sigma_x, \sigma_y, \sigma_z)$ are the Pauli matrices, $\hat{\mathbf{I}}$ and $\hat{\mathbf{k}}_n$ are unit vectors along the nuclear spin and the neutron momentum, respectively. The coefficients α , $\beta_{\hat{\mathbf{I}}}$, $\beta_{\hat{\mathbf{k}}_n}$, and $\beta_{\hat{\mathbf{k}}_n \times \hat{\mathbf{I}}}$ denote one spin-independent amplitude and three spin-correlation amplitudes. In particular, the $\beta_{\hat{\mathbf{k}}_n \times \hat{\mathbf{I}}}$ component is odd under both parity and time reversal transformations, making it a clean signature of TRIV effects where fake TRIV effects, commonly referred to as the final state interaction or nuclear recoil effects, are experimentally controllable by suppressing and/or varying contamination of non-forward scattering neutrons.

In neutron-induced compound nuclear processes, parity violating (PV) effects as large as 10^{-2} – 10^{-1} have been observed in p -wave resonances near s -wave tails, representing enhancements of up to six orders of magnitude compared to PV effects in nucleon-nucleon interactions [4–8]. This enhancement can be interpreted as a statistical amplification of many small contributions, arising from the large number of degrees of freedom in compound nuclei [9–13]. A similar mechanism is expected to enhance TRIV effects as well [9, 11, 12]. A quantitative connection between TRIV and PV cross sections is established via a spin-dependent factor $\kappa(J)$, which depends on the spin of the compound nucleus and on the partial neutron widths of p -wave resonances [10, 14]. The TRIV and PV cross sections, $\Delta\sigma_{\mathcal{TP}}$ and $\Delta\sigma_{\mathcal{P}}$, are related by

$$\Delta\sigma_{\mathcal{TP}} = \kappa(J) \frac{W_T}{W} \Delta\sigma_{\mathcal{P}}, \quad (2)$$

where W_T and W denote the TRIV and PV matrix elements of the nucleon-nucleon interaction, respectively [9]. For a compound nuclear spin $J = I + 1/2$, the value of $\kappa(J)$ is given

by [15]

$$\kappa(J) = \frac{I}{I+1} \left(1 + \frac{1}{2} \sqrt{\frac{2I+3}{I}} \frac{y}{x} \right), \quad (3)$$

where I is the spin of the target nucleus. Here, x and y represent the ratios of p -wave neutron widths for total angular momentum $j = 1/2$ and $j = 3/2$ to the p -wave width Γ_p^n . They are defined as $x^2 = \Gamma_{p,j=1/2}^n / \Gamma_p^n$ and $y^2 = \Gamma_{p,j=3/2}^n / \Gamma_p^n$ [16], satisfying $x^2 + y^2 = 1$. A corresponding mixing angle ϕ can therefore be defined via $x = \cos \phi$ and $y = \sin \phi$.

As seen in Eq. 2, the sensitivity to TRIV effects is proportional to the product $\Delta\sigma_p \kappa(J)$. This highlights the importance of choosing an optimal target nucleus. Previous measurements have reported a longitudinal asymmetry of $9.55 \pm 0.35\%$ in the neutron absorption reaction of ^{139}La at a 0.75 eV p -wave resonance [6]. The combination of a large PV effect and a low resonance energy makes ^{139}La a particularly attractive candidate. Moreover, the value of $\kappa(J)$ for ^{139}La has been experimentally determined to be 0.59 ± 0.05 [17]. Given these favorable characteristics, the search for TRIV effects in neutron transmission using ^{139}La has entered a new phase. However, several challenges remain to be addressed in the high-sensitivity search for TRIV effects in transmission experiments. One is the technical difficulty of controlling neutron and nuclear spins in transmission geometry, and the other is the development of a rigorous theoretical framework.

In this study, we derive a constraint on TRIV effects by applying the density matrix formalism for neutron spin propagation to the transmission data reported in Ref. [18], incorporating the forward scattering amplitude of ^{139}La expanded up to third-rank tensor polarizations. The data employed in this analysis were not optimized for P-odd/T-odd observables but were originally obtained from an experiment aimed at measuring the spin-dependent cross section at the p -wave resonance. Accordingly, it is important to emphasize that the sensitivity to W_T/W is intrinsically orders of magnitude lower than that achievable in future dedicated experiments. Preliminary results were previously reported in the proceedings [19] (in press). This paper provides a complete theoretical treatment and quantitative analysis extending that work. It demonstrates the applicability of the theoretical framework to experimental data and supports the determination of the required precision of spectroscopic parameters for future high-sensitivity searches.

2 Spin observables in transmission through polarized ^{139}La

2.1 Optical description of neutron spin behavior

To describe the spin-dependent observables in neutron transmission, we adopt the density matrix formalism for neutron spin propagation in a coordinate system where the z -axis

is taken parallel to the momentum of incident neutrons. The orientation of the nuclear spin is specified by the polar and azimuthal angles (ϑ_I, φ_I) , as illustrated in Fig. 1. The corresponding expressions for the neutron wave vector, nuclear spin, and their cross product are given by

$$\hat{\mathbf{k}}_n = \begin{pmatrix} 0 \\ 0 \\ 1 \end{pmatrix}, \quad \hat{\mathbf{I}} = \begin{pmatrix} \sin \vartheta_I \cos \varphi_I \\ \sin \vartheta_I \sin \varphi_I \\ \cos \vartheta_I \end{pmatrix}, \quad \hat{\mathbf{k}}_n \times \hat{\mathbf{I}} = \begin{pmatrix} -\sin \vartheta_I \sin \varphi_I \\ \sin \vartheta_I \cos \varphi_I \\ 0 \end{pmatrix}. \quad (4)$$

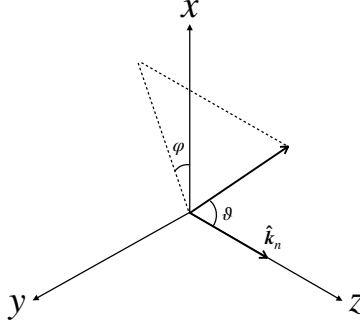


Fig. 1 Experimental coordinate system defined by polar angle ϑ and azimuthal angle φ . The neutron momentum is fixed along the z -axis.

The effective Hamiltonian in the two-dimensional neutron spin space is expressed as the sum of the Fermi pseudopotential and the interaction with an external magnetic field:

$$H = -\frac{2\pi\hbar^2}{m_n}\rho f - \boldsymbol{\mu}_n \cdot \mathbf{B}_{\text{ext}}, \quad (5)$$

where \mathbf{B}_{ext} denotes the external magnetic field, which is aligned with the nuclear spin direction. Here, m_n is the neutron mass, μ_n is the neutron magnetic moment, and ρ is the number density of target nuclei. Following Ref. [20], the non-unitary spin-propagation operator \mathfrak{S} for a neutron propagating through a polarized target of thickness z and velocity v_n is given by

$$\mathfrak{S} = \exp\left(-\frac{iHz}{v_n\hbar}\right) = \exp\left[iZ\left(\alpha + \boldsymbol{\sigma}_n \cdot \tilde{\boldsymbol{\beta}}\right)\right], \quad (6)$$

where $Z \equiv 2\pi\rho z/k_n$ denotes a wavenumber weighted column density that converts the forward scattering amplitude into dimensionless spin-rotation/spin-dependent attenuation factors in the operator. We introduce $\tilde{\boldsymbol{\beta}}$ as the spin correlation amplitude including an

effective scattering length due to the external magnetic field, defined as

$$\tilde{\boldsymbol{\beta}} = \begin{pmatrix} (\beta_{\hat{\mathbf{I}}} - \mu_{\text{eff}} B_{\text{ext}}) \sin \vartheta_I \cos \varphi_I - \beta_{\hat{\mathbf{k}}_n \times \hat{\mathbf{I}}} \sin \vartheta_I \sin \varphi_I \\ (\beta_{\hat{\mathbf{I}}} - \mu_{\text{eff}} B_{\text{ext}}) \sin \vartheta_I \sin \varphi_I + \beta_{\hat{\mathbf{k}}_n \times \hat{\mathbf{I}}} \sin \vartheta_I \cos \varphi_I \\ \beta_{\hat{\mathbf{k}}_n} + (\beta_{\hat{\mathbf{I}}} - \mu_{\text{eff}} B_{\text{ext}}) \cos \vartheta_I \end{pmatrix}, \quad \tilde{\beta} = \sqrt{\tilde{\beta}_x^2 + \tilde{\beta}_y^2 + \tilde{\beta}_z^2}, \quad (7)$$

where $\mu_{\text{eff}} \equiv -m_n \mu_n / (2\pi \hbar^2 \rho)$ is the effective magnetic moment in the target. We write all three-vectors as column vectors in the Cartesian basis (x, y, z) . Using the exponential identity for spin operators, Eq. 6 becomes

$$\mathfrak{S} = e^{iZ\alpha} \left[\cos(Z\tilde{\beta}) + iZ \frac{\sin(Z\tilde{\beta})}{Z\tilde{\beta}} \boldsymbol{\sigma}_n \cdot \tilde{\boldsymbol{\beta}} \right], \quad (8)$$

which leads to the matrix form

$$\mathfrak{S} = \begin{pmatrix} A + C & B - iD \\ B + iD & A - C \end{pmatrix}, \quad (9)$$

with

$$A = e^{iZ\alpha} \cos(Z\tilde{\beta}), \quad B = iZ e^{iZ\alpha} \frac{\sin(Z\tilde{\beta})}{Z\tilde{\beta}} \tilde{\beta}_x, \quad C = iZ e^{iZ\alpha} \frac{\sin(Z\tilde{\beta})}{Z\tilde{\beta}} \tilde{\beta}_z, \quad D = iZ e^{iZ\alpha} \frac{\sin(Z\tilde{\beta})}{Z\tilde{\beta}} \tilde{\beta}_y. \quad (10)$$

The common factor $e^{iZ\alpha}$ governs the total transmittance. The spin-dependent components (B, C, D) are modulated by the suppression factor $\sin(Z\tilde{\beta})/Z\tilde{\beta}$, representing spin precession around the respective axes. Notably, this suppression is sensitive to the external magnetic field, since the term $\mu_{\text{eff}} B_{\text{ext}}$ typically dominates over $\text{Re}\beta_{\hat{\mathbf{I}}}$.

2.2 Expectation value of transmission and observed asymmetry

The neutron transmission probability, normalized to the number of incident neutrons, is derived from the propagation of the density matrix under the operator \mathfrak{S} for an initially polarized neutron ensemble. Let $(\vartheta_\sigma, \varphi_\sigma)$ denote the polar and azimuthal angles of the initial neutron spin orientation in the coordinate system shown in Fig. 1. Then, the initial spin density matrix with polarization degree $p_0 \geq 0$ is given by

$$\hat{\rho} = \frac{1}{2} \begin{pmatrix} 1 + p_z & p_x - ip_y \\ p_x + ip_y & 1 - p_z \end{pmatrix}, \quad (11)$$

where the polarization components are defined as:

$$p_x = p_0 \sin \vartheta_\sigma \cos \varphi_\sigma, \quad p_y = p_0 \sin \vartheta_\sigma \sin \varphi_\sigma, \quad p_z = p_0 \cos \vartheta_\sigma. \quad (12)$$

Let $\hat{\rho}_+$ and $\hat{\rho}_-$ denote the density matrices corresponding to spin-up and spin-down initial states, respectively. The transmission probabilities N_+ and N_- for spin-up and spin-down

initial states, respectively, are calculated using Eqs. 8 and 11 as follows:

$$\begin{aligned}
N_+ &= \text{Tr}(\mathfrak{S}\hat{\rho}_+\mathfrak{S}^\dagger) \\
&= |A|^2 + |B|^2 + |C|^2 + |D|^2 \\
&\quad + 2p_x [\text{Re}(A^*B) + \text{Im}(C^*D)] + 2p_y [\text{Re}(A^*D) + \text{Im}(B^*C)] + 2p_z [\text{Re}(A^*C) + \text{Im}(D^*B)], \\
N_- &= \text{Tr}(\mathfrak{S}\hat{\rho}_-\mathfrak{S}^\dagger) \\
&= |A|^2 + |B|^2 + |C|^2 + |D|^2 \\
&\quad - 2p_x [\text{Re}(A^*B) + \text{Im}(C^*D)] - 2p_y [\text{Re}(A^*D) + \text{Im}(B^*C)] - 2p_z [\text{Re}(A^*C) + \text{Im}(D^*B)].
\end{aligned} \tag{13}$$

The total transmission consists of a spin-independent part (the squared norms) and a spin-dependent part, which reverses sign for opposite spin states. The real components are associated with direct attenuation from spin-dependent absorption, whereas the imaginary components arise from secondary polarization effects accumulated during transmission through the polarized target. The observed asymmetry, or analyzing power $A_I(\vartheta_{kI})$, is defined as:

$$\begin{aligned}
A_I(\vartheta_{kI}) &= \frac{N_+ - N_-}{N_+ + N_-} \\
&= \frac{2p_x [\text{Re}(A^*B) + \text{Im}(C^*D)] + 2p_y [\text{Re}(A^*D) + \text{Im}(B^*C)] + 2p_z [\text{Re}(A^*C) + \text{Im}(D^*B)]}{|A|^2 + |B|^2 + |C|^2 + |D|^2}.
\end{aligned} \tag{14}$$

This expression shows that, by aligning the neutron spin along an appropriate direction, one can selectively access a desired component of the scattering amplitude in Eq. 1. As pointed out in Ref. [12], the second-order contributions can be canceled by measuring both the asymmetry and the resulting polarization $P_I(\vartheta_{kI})$, where the imaginary components contribute with opposite signs. For instance, choosing the spin orientation $(\vartheta_\sigma, \varphi_\sigma) = (\pi/2, \pi/2)$ to isolate the $\beta_{\hat{\mathbf{k}}_n \times \hat{\mathbf{I}}}$ term, we find

$$\frac{A_I(\vartheta_{kI})}{p_{0,a}} + \frac{P_I(\vartheta_{kI})}{p_{0,p}} = \frac{4 \text{Re}(A^*D)}{|A|^2 + |B|^2 + |C|^2 + |D|^2}, \tag{15}$$

where $p_{0,a}$ and $p_{0,p}$ represent the analyzing power and polarization efficiencies, respectively. The interference term A^*X_i and $X_i^*X_j$ for $X_{i(j \neq i)} = B, D, C$ is expressed as

$$\begin{aligned}
A^*X_i &= \frac{e^{-2 \text{Im}(Z\alpha)}}{2|\tilde{\beta}|^2} \left[i \sin(2 \text{Re}(Z\tilde{\beta})) - \sinh(2 \text{Im}(Z\tilde{\beta})) \right] \tilde{\beta}^* \tilde{\beta}_i \\
X_i^*X_j &= \frac{e^{-2 \text{Im}(Z\alpha)}}{2|\tilde{\beta}|^2} \left[i \cos(2 \text{Re}(Z\tilde{\beta})) + \cosh(2 \text{Im}(Z\tilde{\beta})) \right] \tilde{\beta}_i^* \tilde{\beta}_j
\end{aligned} \tag{16}$$

and the sum of squared norms as

$$\begin{aligned}
& |A|^2 + |B|^2 + |C|^2 + |D|^2 \\
&= \frac{e^{-2\text{Im}(Z\alpha)}}{2} \left[\cos(2\text{Re}(Z\tilde{\beta})) + \cosh(2\text{Im}(Z\tilde{\beta})) + \frac{-\cos(2\text{Re}(Z\tilde{\beta})) + \cosh(2\text{Im}(Z\tilde{\beta}))}{|\tilde{\beta}|^2} \sum_i |\tilde{\beta}_i|^2 \right],
\end{aligned} \tag{17}$$

where $i = x, y, z$ and corresponding $X_i = B, D, C$. In the ideal case where $|\sin(Z\tilde{\beta})/Z\tilde{\beta}| = 1$ holds (i.e., perfect control over the pseudomagnetic field), Eq. 15 reduces to the conventional result:

$$\frac{A_I(\vartheta_{kI})}{p_{0,a}} + \frac{P_I(\vartheta_{kI})}{p_{0,p}} = -2 \tanh(2\text{Im}(Z\tilde{\beta}_y)) \approx -4Z\text{Im}\beta_{\hat{\mathbf{k}}_n \times \hat{\mathbf{I}}}. \tag{18}$$

This expression demonstrates that the combined asymmetry is directly related to the TRIV observable $\Delta\sigma_{\mathcal{T}p}$, the primary quantity probed by the NOPTREX collaboration.

2.3 Forward scattering amplitude of ^{139}La

In previous sections, the forward scattering amplitude was formulated using four spin-correlation terms. However, for the specific case of the target nucleus ^{139}La with spin $I = 7/2$, contributions from higher-rank spherical tensors must be included. For low-energy neutrons, contributions from higher orbital angular momenta ($l > 1$) are negligible, and only terms with tensor ranks $q \leq 3$ need to be considered. The forward scattering amplitude for ^{139}La , incorporating tensor polarizations up to rank 3, is given in Ref. [21] as:

$$\begin{aligned}
\alpha &= A' + P_1 H'(\hat{\mathbf{k}}_n \cdot \hat{\mathbf{I}}) + P_2 E' \left[(\hat{\mathbf{k}}_n \cdot \hat{\mathbf{I}})^2 - \frac{1}{3} \right], \\
\beta_{\hat{\mathbf{I}}} &= P_1 B' + P_2 F'(\hat{\mathbf{k}}_n \cdot \hat{\mathbf{I}}) + P_3 \frac{B'_3}{3} \left[(\hat{\mathbf{k}}_n \cdot \hat{\mathbf{I}})^2 - 1 \right], \\
\beta_{\hat{\mathbf{k}}_n} &= C' + P_1 K'(\hat{\mathbf{k}}_n \cdot \hat{\mathbf{I}}) - \frac{1}{3} P_2 F' + \frac{2}{3} P_3 B'_3(\hat{\mathbf{k}}_n \cdot \hat{\mathbf{I}}), \quad \beta_{\hat{\mathbf{k}}_n \times \hat{\mathbf{I}}} = P_1 D'.
\end{aligned} \tag{19}$$

Here, P_1 , P_2 , and P_3 are the tensor polarization components of rank 1, 2, and 3, respectively. Additional coefficients, H' , K' , E' , F' , and B'_3 , proportional to the inner product of neutron momentum and nuclear spin are added to the scattering amplitude. The primed coefficients are calculated using the two-resonance approximation including s - and p -wave

states, as described in Ref. [21] as

$$\begin{aligned}
A' &= -\frac{1}{32k_n}(9t_{s0} + 7t_{s1} + 9t_p) + \frac{i}{16}(9t_{s0}a_{s0} + 7t_{s1}a_{s1}) - \frac{1}{16}(9a_{s0} + 7a_{s1}) + \frac{ik_n}{16}(9a_{s0}^2 + 7a_{s1}^2) \\
B' &= -\frac{1}{32k_n}\left(7t_{s0} - 7t_{s1} + t_p\left(-7x^2 - 2\sqrt{35}xy + \frac{2}{5}y^2\right)\right) \\
&\quad + \frac{i}{16}(7t_{s0}a_{s0} - 7t_{s1}a_{s1}) - \frac{7}{16}(a_{s0} - a_{s1}) + \frac{7ik_n}{16}(a_{s0}^2 - a_{s1}^2), \\
C' &= -\frac{9xW}{16k_n}t_{s0,p}, \quad D' = -\frac{\sqrt{7}W_T}{16k_n}(\sqrt{7}x + \sqrt{5}y)t_{s0,p}, \quad H' = -\frac{\sqrt{21}W}{16k_n}(\sqrt{7}x - 2\sqrt{5}y)t_{s0,p}, \\
K' &= -\frac{1}{16k_n}\left(7x^2 - \sqrt{35}xy - \frac{1}{10}y^2\right)t_p, \\
E' &= \frac{9}{320k_n}\left(4\sqrt{35}xy - 13y^2\right)t_p, \quad F' = \frac{9\sqrt{35}yW}{80k_n}t_{s0,p}, \quad B'_3 = \frac{81y^2}{320k_n}t_p,
\end{aligned} \tag{20}$$

where t_{s0} , t_{s1} , and t_p are Breit-Wigner amplitude formulae for the negative s -wave, s -wave at the 72 eV, and p -wave resonances, written as

$$t_{s0} = \frac{\Gamma_{s0}^n}{E - E_{s0} + i\Gamma_{s0}/2}, \quad t_{s1} = \frac{\Gamma_{s1}^n}{E - E_{s1} + i\Gamma_{s1}/2}, \quad t_p = \frac{\Gamma_p^n}{E - E_p + i\Gamma_p/2}, \tag{21}$$

and $t_{s0,p}$ is

$$t_{s0,p} = \frac{\sqrt{\Gamma_{s0}^n}\sqrt{\Gamma_p^n}}{(E - E_p + i\Gamma_p/2)(E - E_{s0} + i\Gamma_{s0}/2)}. \tag{22}$$

The resonance parameters E_K , Γ_K^n , and Γ_K are the resonance energy, neutron width, and total width of K th resonance. The potential scattering lengths of the s_0 - and s_1 -waves are a_{s0} and a_{s1} , respectively. Since the spin coupling schemes differ between Eq. 3 and Refs. [15, 21], a conversion is applied to relate the two conventions, $x_S = -\frac{1}{2\sqrt{3}}(\sqrt{7}x + \sqrt{5}y)$ and $y_S = \frac{1}{2\sqrt{3}}(\sqrt{5}x - \sqrt{7}y)$. Thus, it is demonstrated that we can analyze numerical calculation of the observed quantity in Eq. 14 by substituting the resonance parameters into Eq. 20.

3 Evaluation of the TRIV upper limit

3.1 Interpretation of the previous experiment

A previous transmission experiment conducted by the NOPTREX collaboration [18] measured the spin-dependent cross section at the 0.75 eV p -wave resonance using polarized neutrons transmitted through a transversely polarized ^{139}La target. Although the scalar triple product $\boldsymbol{\sigma}_n \cdot (\hat{\mathbf{k}}_n \times \hat{\mathbf{I}})$ vanishes in this experimental configuration, a small contribution from the $\beta_{\hat{\mathbf{k}}_n \times \hat{\mathbf{I}}}$ can still contribute via second-order leakage of spin precession. We

evaluate TRIV effects in dataset from Ref. [18] using the developed formulae as shown in Eqs. 14 and 20.

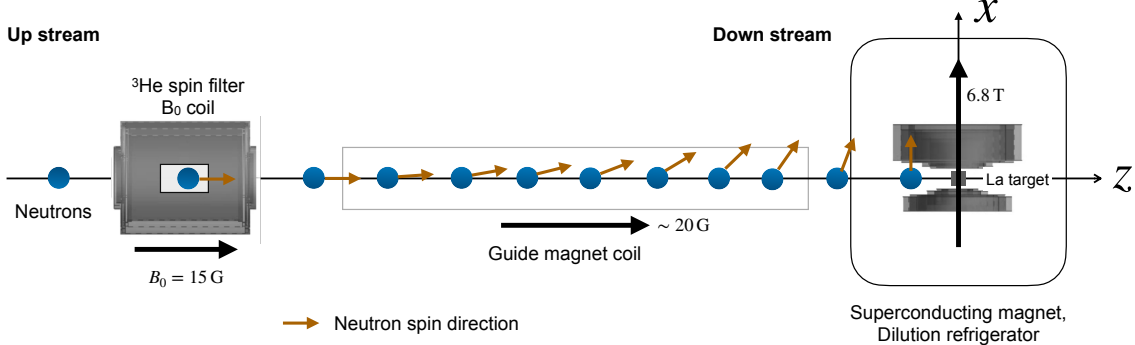


Fig. 2 Schematic layout of the polarized-neutron transmission experiment through a transversely polarized ^{139}La target. The incident pulsed neutron beam was polarized by a ^3He spin filter and guided into the superconducting magnet surrounding the lanthanum metal cube. After passing through the 2.0 cm cube, the transmitted neutrons are detected for parallel and antiparallel relative to the target polarization.

The experiment was performed using a pulsed neutron beam at the RADEN beam-line [22], located at the Material and Life Science Experimental Facility (MLF) [23] at the Japan Proton Accelerator Research Complex (J-PARC). The incident neutron beam was polarized with the ^3He spin filter device [24] and the averaged neutron polarization \bar{p}_0 was $36.1 \pm 0.5\%$ at the neutron energy of 0.75 eV. A 2.0 cm cube of lanthanum metal target was employed and cooled with a dilution refrigerator. Figure 2 shows the experimental system in which a polarized neutron beam propagates through the polarized target. A transverse magnetic field $|\mathbf{B}_{\text{ext}}| = 6.8 \text{ T}$ was applied and the target temperature was determined to be $75.7^{+10.2}_{-8.9} \text{ mK}$. Therefore, P_1 , P_2 , and P_3 were obtained to be $3.9 \pm 0.5\%$, $0.1^{+0.03}_{-0.02}\%$, and $(2.1 \pm 1.0) \times 10^{-3}\%$, respectively. The beam divergence $(\hat{\mathbf{k}}_n \cdot \hat{\mathbf{I}})$ in Eq. 19 was below 2×10^{-3} taking into account the maximum angle on flight path. Polarized neutrons passing through the polarized target were counted for parallel and antiparallel spin orientations between the neutrons and the target, denoted N_+ and N_- . The experimental asymmetry was quantified using the analyzing power, defined as

$$(A_I(\vartheta_{kI}))_{\text{exp}} = \frac{1}{\bar{p}_0} \frac{N_- - N_+}{N_- + N_+}, \quad (23)$$

where the number of transmitted neutrons was counted using the time-of-flight (TOF) method. The relation between an incident neutron energy and TOF was calculated as

E (eV) = 5.227×10^{-3} (LOF (m)/TOF)² (ms), where LOF (length-of-flight) was 24.713 m. We set the experimental coordinate angles to $(\vartheta_I, \varphi_I) = (\pi/2, 0)$ and $(\vartheta_\sigma, \varphi_\sigma) = (\pi/2, 0)$, because the ratio of the perturbing field to $|\mathbf{B}_{\text{ext}}|$ was conservatively estimated to be below 10^{-4} . Therefore, the analyzing power can be calculated from Eq. 14 as

$$A_I(\vartheta_{kI}) = -\frac{2 [\text{Re}A^*B + \text{Im}C^*D]}{|A|^2 + |B|^2 + |C|^2 + |D|^2}, \quad (24)$$

where $\tilde{\beta}$ can be expressed as

$$\tilde{\beta} = \begin{pmatrix} \beta_{\hat{I}} - \mu_{\text{eff}} B_{\text{ext}} \\ \beta_{\hat{\mathbf{k}}_n \times \hat{I}} \\ \beta_{\hat{\mathbf{k}}_n} \end{pmatrix}, \quad \tilde{\beta} = \sqrt{(\beta_{\hat{I}} - \mu_{\text{eff}} B_{\text{ext}})^2 + \beta_{\hat{\mathbf{k}}_n \times \hat{I}}^2 + \beta_{\hat{\mathbf{k}}_n}^2}. \quad (25)$$

Here, we evaluate which spin correlation terms dominate in Eq. 24. As shown in Eqs. 16 and 17, when $\sum_i |\tilde{\beta}_i|^2 / |\tilde{\beta}|^2 \simeq 1$ holds, the second-order contribution of $\tilde{\beta}$ can be neglected, and it suffices to keep only the first-order term. Because it is naturally considered to be $|D'| \ll |B'|$, it follows $|\tilde{\beta}_y|^2 \ll |\tilde{\beta}_x|^2$. Then a numerical estimate around the p -wave resonance was computed to be $|\tilde{\beta}_z|^2 / \sum_i |\tilde{\beta}_i|^2 = 4 \times 10^{-11}$. During the computation of spin correlation

Table 1 Resonance parameters of ^{139}La reported by Endo *et al.* (2023). [25]

K	E_K (eV)	J_K	l_K	Γ_K^γ (meV)	$g_K \Gamma_K^n$ (meV)	
0	-38.8 ± 0.4	4	0	60.3 ± 0.5	346 ± 10	s_0
1	0.750 ± 0.001	4	1	41.6 ± 0.9	$(3.67 \pm 0.05) \times 10^{-5}$	p
2	72.30 ± 0.01	3	0	64.1 ± 3.0	13.1 ± 0.7	s_1

terms B', C', K', F' , and B'_3 , we chose the mixing angle ϕ to maximize each term individually and the P-odd matrix element was taken to be $W \sim 1$ meV in Refs. [26–28], and all resonance parameters and physical constants were taken to be the same as in Ref. [18] as listed in Tab. 1. The second term, $\text{Im}C^*D$, vanishes because the resonance $R_{s0,p}$ is common to both, giving $\text{Im}C'^*D' = 0$. Moreover, as shown below, the contributions from spin correlation terms other than C' are entirely negligible. Consequently, we thus obtain $\text{Re}A^*B \propto \sinh(2\text{Im}(Z\tilde{\beta}))$ and $|A|^2 + |B|^2 + |C|^2 + |D|^2 \propto \cosh(2\text{Im}(Z\tilde{\beta}))$. Therefore, Eq. 24 can be obtained as

$$A_I(\vartheta_{kI}) = -\tanh(2\text{Im}(Z\tilde{\beta})). \quad (26)$$

To identify the dominant contribution to the first-order $\text{Im}(Z\tilde{\beta})$, we examined the residual of the ratio between computations with and without each spin correlation term. Table 2

Table 2 Residual from unity of the ratio computed by excluding a specific correlation term included in $\text{Im}\tilde{\beta}$. Since the real part of the resonance enters in differential form, $\text{Im}\tilde{\beta}$ was evaluated using the value integrated over $\pm 3\Gamma_p$ around the p -wave resonance.

η	$P_1 B' = 0$	$\mu_{\text{eff}} B_{\text{ext}} = 0$	$C' = 0$	$P_2 F' = 0$	$P_1 K'(\hat{\mathbf{k}}_n \cdot \hat{\mathbf{I}}) = 0$	$P_3 B'_3 = 0$
$1 - \frac{\text{Im}\tilde{\beta}(\eta)}{\text{Im}\tilde{\beta}}$	1	0.9	2×10^{-6}	1×10^{-4}	2×10^{-8}	2×10^{-4}

presents the numerical results: contributions proportional to tensor polarizations of second and third rank, to the beam divergence, and to the P-odd term C' were all below 10^{-4} . Considering that the spin-dependent cross section at the p -wave resonance was obtained as a statistical relative uncertainty of 0.3 [18], we can therefore approximate

$$\tilde{\beta} \simeq \sqrt{(P_1 B' - \mu_{\text{eff}} B_{\text{ext}})^2 + (P_1 D')^2}. \quad (27)$$

To clarify the contribution of the D' term, we expand $\text{Im}\tilde{\beta}$. In the regime where the external magnetic field dominates, it can be approximated as $\text{Im}\tilde{\beta} \simeq P_1 \text{Im}B' + \frac{P_1^2 \text{Re}D' \text{Im}D'}{\mu_{\text{eff}} B_{\text{ext}}}$. This shows that the observable TRIV contribution is suppressed by the inverse of the external magnetic field and scales with the square of the nuclear polarization.

3.2 Evaluation of TRIV Effects

The global structure of the measured asymmetry $(A_I(\vartheta_{kI}))_{\text{exp}}$, shown in the upper panel of Fig. 3, is primarily governed by s_0 - and s_1 -wave resonances, which originate from the independent potential scattering lengths a_{s0} and a_{s1} in the B' term. To isolate the p -wave contribution, we subtract this s -wave background using a third-order polynomial fitted to the regions outside the three resonances. Let $(A_I(\vartheta_{kI}))_{\text{sub}}$ denote the residual asymmetry after subtracting this global structure. The corresponding theoretical expression around the p -wave resonance is given using Eqs. 26 and 27 by

$$A_I(\vartheta_{kI})_{\text{sub}}(E; W_T, \phi, E_p) = -\tanh\left(2\text{Im}(Z\tilde{\beta}_p)\right), \quad (28)$$

$$\tilde{\beta}_p = \sqrt{(P_1 B'_p(E; \phi, E_p) - \mu_{\text{eff}} B_{\text{ext}})^2 + (P_1 D'(E; W_T, \phi, E_p))^2},$$

where $B'_p = -\frac{1}{32k_n} t_p (-7x^2 - 2\sqrt{35}xy + \frac{2}{5}y^2)$, and the product of the atomic number density and target thickness is $\rho z = 0.053 \text{ b}^{-1}$. We used the resonance parameters listed in Tab. 1. As shown in Fig. 3, the fits were performed in the energy region of $E_p \pm 3\Gamma_p$ centered at the p -wave resonance. With the two-parameter fit in (W_T, ϕ) , the data yielded $\chi^2 = 13.0$ for the number degrees of freedom (ndf) of $N_{\text{data}} - 2 = 5$. Although the fit yielded $\chi^2/\text{ndf} = 2.61$ and a p -value of 0.023, which marginally disfavors the model, the discrepancy

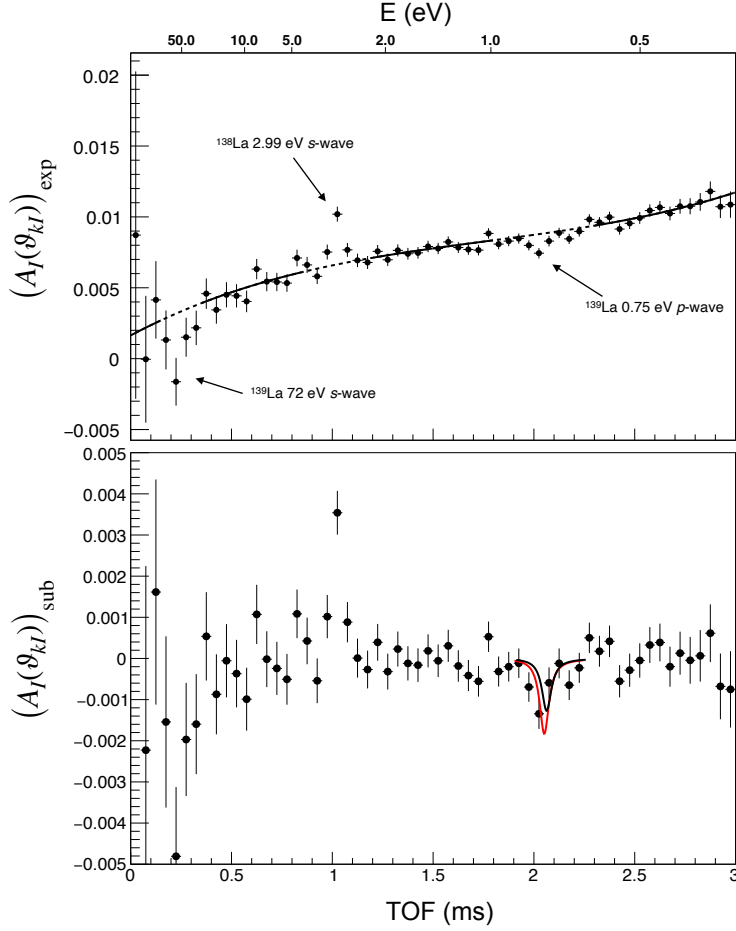


Fig. 3 Upper panel: Measured asymmetry $(A_I(\vartheta_{kI}))_{\text{exp}}$ (corrected for neutron polarization) as a function of TOF or corresponding neutron energy. Black solid line represents the third-order polynomial fit to the regions outside the three known resonances. Note that the 2.99 eV s -wave resonance arises from 0.09% ^{138}La impurity ($J = 11/2$). Lower panel: Residual asymmetry $(A_I(\vartheta_{kI}))_{\text{sub}}$ after subtracting the third polynomial background, overlaid with the two best-fit curves. The black line represents the curve with W_T and ϕ as free parameters and $E_p = 0.750\text{ eV}$ fixed, while the red line represents the results obtained by searching for the global minimum with E_p as a nuisance parameter and then executing with two parameters (details are described in the main text). The fitting range is $E_p \pm 3\Gamma_p$ (approximately TOF = 1.91 to 2.26 ms).

is not conclusive. Hence, assuming that the excess χ^2 can be attributed to a shift in the p -wave resonance energy, the resonance energy E_p was treated as a constrained nuisance parameter [29] using a Gaussian pull term based on external measurements, which were used as five independent measurements listed in Tab. 3. An empirical prior of $E_p = 0.749 \pm 0.005$

Table 3 p -wave resonance energies reported in the literature.

	E_p (eV)		E_p (eV)
Harvey <i>et al.</i> (1959) [30]	0.752 ± 0.011	Terlizzi <i>et al.</i> (2007) [31]	0.758 ± 0.001
Shwe <i>et al.</i> (1967) [32]	0.734 ± 0.005	Endo <i>et al.</i> (2023) [25]	0.750 ± 0.001
Alfimenkov <i>et al.</i> (1983) [4]	0.750 ± 0.010		

eV was derived as the unweighted mean μ_{E_p} and its standard deviation σ_{E_p} , because the quoted errors are not directly comparable across experiments. Therefore, three-parameter chi-square formula can be obtained as

$$\chi^2(W_T, \phi, E_p) = \sum_i \frac{[(A_I(\vartheta_{kI}))_{\text{sub},i} - A_I(\vartheta_{kI})_{\text{sub}}(E_i; W_T, \phi, E_p)]^2}{\sigma_i^2} + \frac{(E_p - \mu_{E_p})^2}{\sigma_{E_p}^2}, \quad (29)$$

where the second term represents the Gaussian constraint on E_p , effectively incorporating external experimental knowledge into the fit. The global minimum was found at $E_p = 0.758$ eV, for which the data term alone gave $\chi^2_{\text{data}}/\text{ndf} = 7.3/5 = 1.47$ and p -value of 0.20. The pull term, $(0.758 - \mu_{E_p})/\sigma_{E_p} = 1.68$, indicates that the fitted value is still consistent with the external information. Thus the previous overdispersion is largely absorbed by a systematic shift of E_p . Fixing E_p to its best-fit value and profiling over ϕ , we obtained the $\chi^2(W_T, \phi)$ contour map shown in Fig. 4. The solid contours correspond to $\Delta\chi^2 = 2.30$ (68% C.L.) and 4.61 (90% C.L.). The fact that ϕ has four local minima is consistent with the four possible solutions shown in Ref. [18]. The previous studies using (n, γ) reaction measurements [33–35] strongly support that the physical solution is constrained on the second quadrant. With E_p fixed at the best-fit value and its ϕ , fitting with two free parameters of W_T and ϕ yielded $\phi = (161 \pm 3)^\circ$, which is fully consistent with our earlier result of $\phi = (164 \pm 4)^\circ$ [17]. Using these best-fit parameters, we obtained $|W_T| < 6.4$ eV with 90% C.L. and the TRIV cross section was estimated by averaging over the energy region $E_p(\text{best-fit}) \pm 3\Gamma_p$, yielding $|\Delta\sigma_{\text{TRIV}}| < 1.2 \times 10^2$ b.

4 Conclusion

We have extended the density matrix formalism for polarized-neutron transmission through transversely polarized ^{139}La taking into account the explicit forward scattering amplitude. Applying the formalism to existing transmission data, we obtained $|W_T| < 6.4$ eV, $|\Delta\sigma_{\text{TRIV}}| < 1.2 \times 10^2$ b with 90% C.L. Although the sensitivity achieved here, expressed in terms of W_T , is intrinsically many orders of magnitude lower than the reach

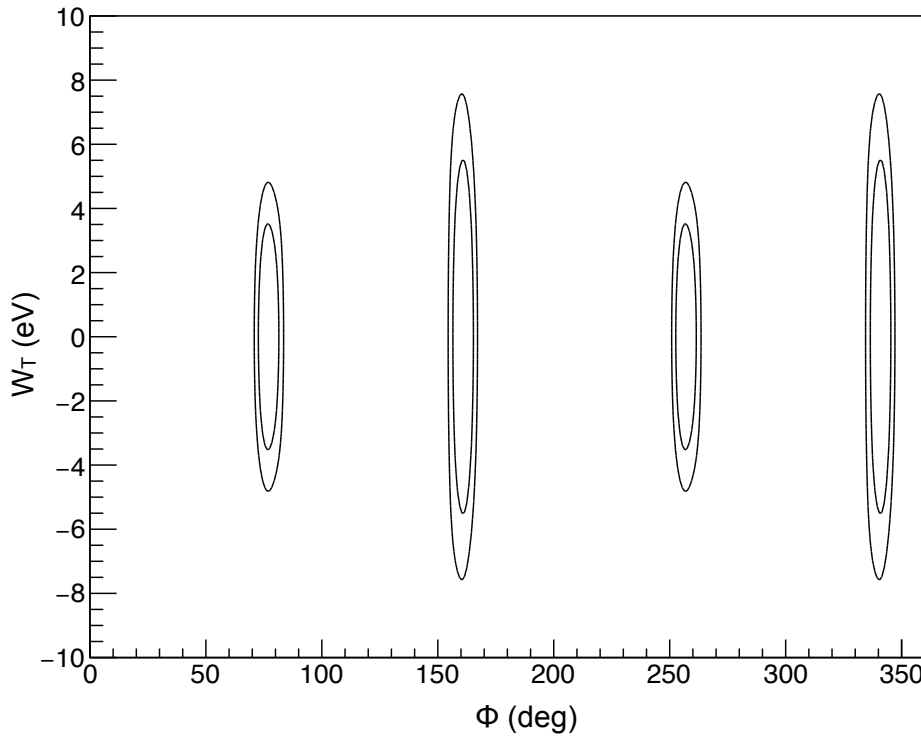


Fig. 4 $\min_{E_p} \chi^2(W_T, \phi)$ contour mapping in the two-parameter fit space. The inner and outer black lines correspond to the 68% C.L. ($\Delta\chi^2 = 2.30$) and 90% C.L. ($\Delta\chi^2 = 4.61$), respectively.

anticipated for future dedicated searches, our analysis validates the methodology on real data and provides practical guidance for optimizing the configuration of next-generation TRIV experiments. For example, the model study in Ref. [12] projects a statistical sensitivity to W_T/W at the level of 10^{-6} ; see also Ref. [36] for a complementary statistical treatment and sensitivity scaling.

Acknowledgment

This work was financially supported by Japan Society for the Promotion of Science KAKENHI Grants No. 17H02889, No. 19K21047, No. 20K14495, No. 23K13122, and No. 24H00222, and No. 25K01024. C. Auton, J. G. Otero-Munoz, and W. M. Snow acknowledge support from US National Science Foundation (NSF) grant PHY-2209481 and the Indiana University Center for Spacetime Symmetries. J. G. Otero-Munoz also acknowledges the support of the National GEM Consortium and the National Science Foundation AGEPE program. C. Auton also acknowledges support from the Japan Society for the Promotion

of Science. The authors would like to thank the staff of beamline No.22, RADEN, MLF, and J-PARC for operating the accelerators and the neutron production target. The neutron experiment was conducted under the user program (Proposal No. 2022A0101).

References

- [1] Leo Stodolsky, Physics Letters B, **172**(1), 5–9 (1986).
- [2] P K Kabir, Phys. Rev. D, **25**(7), 2013–2014 (1982).
- [3] P. K. Kabir, Phys. Rev. D, **37**, 1856–1859 (Apr 1988).
- [4] V. P. Alfimenkov, S. B. Borzakov, Vo Van Thuan, Yu. D. Mareev, L. B. Pikelner, A. S. Khrykin, and E. I. Sharapov, Nucl. Phys. A, **435**, 352 (1983).
- [5] Y. Masuda, T. Adachi, A. Masaike, and K. Morimoto, Nuclear Physics A, **504**(2), 269–276 (1989).
- [6] V. W. Yuan, C. D. Bowman, J. D. Bowman, J. E. Bush, P. P. J. Delheij, C. M. Frankle, C. R. Gould, D. G. Haase, J. N. Knudson, G. E. Mitchell, S. Penttilä, H. Postma, N. R. Roberson, S. J. Seestrom, J. J. Szymanski, and X. Zhu, Phys. Rev. C, **44**, 2187 (1991).
- [7] Hirohiko M. Shimizu, Toshikazu Adachi, Shigeru Ishimoto, Akira Masaike, Yasuhiro Masuda, and Kimio Morimoto, Nucl. Phys. A, **552**, 293 (1993).
- [8] G.E. Mitchell, J.D. Bowman, S.I. Penttila, and E.I. Sharapov, Physics Reports, **354**(3), 157–241 (2001).
- [9] V. E. Bunakov and V. P. Gudkov, Zeitschrift für Physik A Atoms and Nuclei, **308**, 363–364 (1982).
- [10] V. E. Bunakov and V. P. Gudkov, Nuclear Physics A, **401**(1), 93–116 (1983).
- [11] V P Gudkov, Phys. Rep., **212**(2), 77–105 (1992).
- [12] J. David Bowman and Vladimir Gudkov, Phys. Rev. C, **90**, 065503 (Dec 2014).
- [13] O. P. Sushkov and V. V Flambaum, Soviet Phys. Usp., **25**, 1 (1982).
- [14] V. P. Gudkov, Physics Letters B, **243**, 319–322 (1990).
- [15] Vladimir Gudkov and Hirohiko M Shimizu, Phys. Rev. C, **97**(6), 065502 (2018).
- [16] V. V. Flambaum and O. P. Sushkov, Nucl. Phys. A, **435**, 352 (1985).
- [17] R. Nakabe, C. J. Auton, S. Endo, H. Fujioka, V. Gudkov, K. Hirota, I. Ide, T. Ino, M. Ishikado, W. Kambara, S. Kawamura, A. Kimura, M. Kitaguchi, R. Kobayashi, T. Okamura, T. Oku, T. Okudaira, M. Okuizumi, J. G. Otero Munoz, J. D. Parker, K. Sakai, T. Shima, H. M. Shimizu, T. Shinohara, W. M. Snow, S. Takada, R. Takahashi, S. Takahashi, Y. Tsuchikawa, and T. Yoshioka, Phys. Rev. C, **109**, L041602 (Apr 2024).
- [18] T. Okudaira, R. Nakabe, C. J. Auton, S. Endo, H. Fujioka, V. Gudkov, I. Ide, T. Ino, M. Ishikado, W. Kambara, S. Kawamura, R. Kobayashi, M. Kitaguchi, T. Okamura, T. Oku, J. G. Otero Munoz, J. D. Parker, K. Sakai, T. Shima, H. M. Shimizu, T. Shinohara, W. M. Snow, S. Takada, Y. Tsuchikawa, R. Takahashi, S. Takahashi, H. Yoshikawa, and T. Yoshioka, Phys. Rev. C, **109**, 044606 (Apr 2024).
- [19] Rintaro Nakabe et al., A Preliminary Result on Time-Reversal Invariance Violation in Polarized Neutron Transmission through Polarized ^{139}La , In *Proceedings of the J-PARC Symposium 2024* (2024), In press.
- [20] S K Lamoreaux and R Golub, Physical Review D, **50**(9), 5632–5638 (1994).
- [21] Vladimir Gudkov and Hirohiko M. Shimizu, Phys. Rev. C, **102**, 015503 (Jul 2020).
- [22] Takenao Shinohara, Tetsuya Kai, Kenichi Oikawa, Takeshi Nakatani, Mariko Segawa, Kosuke Hiroi, Yuhua Su, Motoki Ooi, Masahide Harada, Hiroshi Ikura, Hirotoshi Hayashida, Joseph D. Parker, Yoshihiro Matsumoto, Takashi Kamiyama, Hirotaka Sato, and Yoshiaki Kiyonagi, Review of Scientific Instruments, **91**(4), 043302 (04 2020).
- [23] Kenji Nakajima, Yukinobu Kawakita, Shinichi Itoh, Jun Abe, Kazuya Aizawa, Hiroyuki Aoki, Hitoshi Endo, Masaki Fujita, Kenichi Funakoshi, Wu Gong, Masahide Harada, Stefanus Harjo, Takanori Hattori, Masahiro Hino, Takashi Honda, Akinori Hoshikawa, Kazutaka Ikeda, Takashi Ino, Toru Ishigaki, Yoshihisa Ishikawa, Hiroki Iwase, Tetsuya Kai, Ryoichi Kajimoto, Takashi Kamiyama, Naokatsu Kaneko, Daichi Kawana, Seiko Ohira-Kawamura, Takuro Kawasaki, Atsushi Kimura, Ryoji Kiyonagi, Kenji Kojima, Katsuhiro Kusaka, Sanghyun Lee, Shinichi Machida, Takatsugu Masuda, Kenji Mishima, Koji Mitamura, Mitsutaka Nakamura, Shoji Nakamura, Akiko Nakao, Tatsuro Oda, Takashi Ohhara, Kazuki Ohishi, Hidetoshi Ohshita, Kenichi Oikawa, Toshiya Otomo, Asami Sano-Furukawa, Kaoru Shibata, Takenao Shinohara, Kazuhiko Soyama, Jun-ichi Suzuki, Kentaro Suzuya, Atsushi Takahara, Shin-ichi Takata, Masayasu Takeda, Yosuke Toh, Shuki Torii, Naoya Torikai, Norifumi L. Yamada, Taro Yamada, Dai Yamazaki, Tetsuya Yokoo, Masao Yonemura, and Hideki Yoshizawa, Quantum Beam Science, **1**(3) (2017).
- [24] T. Okudaira, T. Oku, T. Ino, H. Hayashida, H. Kira, K. Sakai, K. Hiroi, S. Takahashi, K. Aizawa, H. Endo, S. Endo, M. Hino, K. Hirota, T. Honda, K. Ikeda, K. Kakurai, W. Kambara, M. Kitaguchi, T. Oda, H. Ohshita, T. Otomo, H.M. Shimizu, T. Shinohara, J. Suzuki, and T. Yamamoto, Nuclear Instruments and Methods in Physics Research Section A: Accelerators, Spectrometers, Detectors and Associated Equipment, **977**, 164301

(2020).

- [25] Shunsuke Endo, Shiori Kawamura, Takuya Okudaira, Hiromoto Yoshikawa, Gerard Rovira, Atsushi Kimura, Shoji Nakamura, Osamu Iwamoto, and Nobuyuki Iwamoto, *The European Physical Journal A*, **59**(288) (2023).
- [26] C. M. Frankle, J. D. Bowman, J. E. Bush, P. P. J. Delheij, C. R. Gould, D. G. Haase, J. N. Knudson, G. E. Mitchell, S. Penttilä, H. Postma, N. R. Roberson, S. J. Seestrom, J. J. Szymanski, S. H. Yoo, V. W. Yuan, and X. Zhu, *Phys. Rev. Lett.*, **67**, 564–567 (Jul 1991).
- [27] J. D. Bowman, C. D. Bowman, J. E. Bush, P. P. J. Delheij, C. M. Frankle, C. R. Gould, D. G. Haase, J. Knudson, G. E. Mitchell, S. Penttilä, H. Postma, N. R. Roberson, S. J. Seestrom, J. J. Szymanski, V. W. Yuan, and X. Zhu, *Phys. Rev. Lett.*, **65**, 1192–1195 (Sep 1990).
- [28] Pavel Fadeev and Victor V Flambaum, *Phys. Rev. C*, **100**(1), 015504 (2019).
- [29] Particle Data Group, R L Workman, V D Burkert, V Crede, E Klempt, U Thoma, L Tiator, K Agashe, G Aielli, B C Allanach, C Amsler, M Antonelli, E C Aschenauer, D M Asner, H Baer, Sw Banerjee, R M Barnett, L Baudis, C W Bauer, J J Beatty, V I Belousov, J Beringer, A Bettini, O Biebel, K M Black, E Blucher, R Bonventre, V V Bryzgalov, O Buchmuller, M A Bychkov, R N Cahn, M Carena, A Ceccucci, A Cerri, R Sekhar Chivukula, G Cowan, K Cranmer, O Cremonesi, G D’Ambrosio, T Damour, D de Florian, A de Gouvêa, T DeGrand, P de Jong, S Demers, B A Dobrescu, M D’Onofrio, M Doser, H K Dreiner, P Eerola, U Egede, S Eidelman, A X El-Khadra, J Ellis, S C Eno, J Erler, V V Ezhela, W Fetscher, B D Fields, A Freitas, H Gallagher, Y Gershtein, T Gherghetta, M C Gonzalez-Garcia, M Goodman, C Grab, A V Gritsan, C Grojean, D E Groom, M Grünewald, A Gurtu, T Gutsche, H E Haber, Matthieu Hamel, C Hanhart, S Hashimoto, Y Hayato, A Hebecker, S Heinemeyer, J J Hernández-Rey, K Hikasa, J Hisano, A Höcker, J Holder, L Hsu, J Huston, T Hyodo, Al Ianni, M Kado, M Karliner, U F Katz, M Kenzie, V A Khoze, S R Klein, F Krauss, M Kreps, P Križan, B Krusche, Y Kwon, O Lahav, J Laiho, L P Lellouch, J Lesgourgues, A R Liddle, Z Ligeti, C-J Lin, C Lippmann, T M Liss, L Littenberg, C Lourenço, K S Lugovsky, S B Lugovsky, A Lusiani, Y Makida, F Maltoni, T Mannel, A V Manohar, W J Marciano, A Masoni, J Matthews, U-G Meißner, I-A Melzer-Pellmann, M Mikhasenko, D J Miller, D Milstead, R E Mitchell, K Mönig, P Molaro, F Moortgat, M Moskvic, K Nakamura, M Narain, P Nason, S Navas, A Nelles, M Neubert, P Nevski, Y Nir, K A Olive, C Patrignani, J A Peacock, V A Petrov, E Pianori, A Pich, A Piepke, F Pietropaolo, A Pomarol, S Pordes, S Profumo, A Quadt, K Rabbertz, J Rademacker, G Raffelt, M Ramsey-Musolf, B N Ratcliff, P Richardson, A Ringwald, D J Robinson, S Roesler, S Rolli, A Romaniouk, L J Rosenberg, J L Rosner, G Rybka, M G Ryskin, R A Ryutin, Y Sakai, S Sarkar, F Sauli, O Schneider, S Schöner, K Scholberg, A J Schwartz, J Schwiening, D Scott, F Sefkow, U Seljak, V Sharma, S R Sharpe, V Shiltsev, G Signorelli, M Silari, F Simon, T Sjöstrand, P Skands, T Skwarnicki, G F Smoot, A Soffer, M S Sozzi, S Spanier, C Spiering, A Stahl, S L Stone, Y Sumino, M J Syphers, F Takahashi, M Tanabashi, J Tanaka, M Taševský, K Terao, K Terashi, J Terning, R S Thorne, M Titov, N P Tkachenko, D R Tovey, K Trabelsi, P Urquijo, G Valencia, R Van de Water, N Varelas, G Venanzoni, L Verde, I Vivarelli, P Vogel, W Vogelsang, V Vorobyev, S P Wakely, W Walkowiak, C W Walter, D Wands, D H Weinberg, E J Weinberg, N Vermes, M White, L R Wiencke, S Willocq, C G Wohl, C L Woody, W-M Yao, M Yokoyama, R Yoshida, G Zanderighi, G P Zeller, O V Zenin, R-Y Zhu, Shi-Lin Zhu, F Zimmermann, and P A Zyla, *Progress of Theoretical and Experimental Physics*, **2022**(8), 083C01 (08 2022), <https://academic.oup.com/ptep/article-pdf/2022/8/083C01/49175539/ptac097.pdf>.
- [30] J.A.Harvey, R.C.Block, and G.G.Slaughter, *Bull. Am. Phys. Soc.*, **4**, 385 (1959).
- [31] R. Terlizzi, U. Abbondanno, G. Aerts, H. Álvarez, F. Alvarez-Velarde, S. Andriamonje, J. Andrzejewski, P. Assimakopoulos, L. Audouin, G. Badurek, P. Baumann, F. Bečvář, E. Berthoumieux, M. Calviani, F. Calviño, D. Cano-Ott, R. Capote, A. Carrillo de Albornoz, P. Cennini, V. Chepel, E. Chiaveri, N. Colonna, G. Cortes, A. Couture, J. Cox, M. Dahlfors, S. David, I. Dillmann, R. Dolfini, C. Domingo-Pardo, W. Dridi, I. Duran, C. Eleftheriadis, M. Embid-Segura, L. Ferrant, A. Ferrari, R. Ferreira-Marques, L. Fitzpatrick, H. Fraai-Koelbl, K. Fujii, W. Furman, R. Gallino, I. Goncalves, E. Gonzalez-Romero, A. Goverdovski, F. Gramegna, E. Griesmayer, C. Guerrero, F. Gunsing, B. Haas, R. Haight, M. Heil, A. Herrera-Martinez, M. Igashira, S. Isaev, E. Jericha, Y. Kadi, F. Käppeler, D. Karamanis, D. Karadimos, M. Kerveno, V. Ketlerov, P. Koehler, V. Konovalov, E. Kossionides, M. Krčička, C. Lamboudis, H. Leeb, A. Lindote, I. Lopes, M. Lozano, S. Lukic, J. Marganec, L. Marques, S. Marrone, C. Massimi, P. Mastinu, A. Mengoni, P. M. Milazzo, C. Moreau, M. Mosconi, F. Neves, H. Oberhummer, S. O’Brien, J. Pancin, C. Papachristodoulou, C. Papadopoulos, C. Paradela, N. Patronis, A. Pavlik, P. Pavlopoulos, L. Perrot, M. Pignatari, R. Plag, A. Plompen, A. Plukis, A. Poch, C. Pretel, J. Quesada, T. Rauscher, R. Reifarth, M. Rosetti, C. Rubbia, G. Rudolf, P. Rullhusen, J. Salgado, L. Sarchiapone, I. Savvidis, C. Stephan, G. Tagliente, J. L. Tain, L. Tassan-Got, L. Tavora, G. Vannini, P. Vaz, A. Ventura, D. Villamarin, M. C. Vincente, V. Vlachoudis, R. Vlastou, F. Voss, S. Walter, H. Wendler, M. Wiescher, and K. Wisshak, *Phys. Rev. C*, **75**, 035807 (Mar 2007).
- [32] Hla Shwe, R. E. Coté, and W. V. Prestwich, *Phys. Rev.*, **159**, 1050 (1967).
- [33] T. Okudaira, S. Takada, K. Hirota, A. Kimura, M. Kitaguchi, J. Koga, K. Nagamoto, T. Nakao, A. Okada,

- K. Sakai, H. M. Shimizu, T. Yamamoto, and T. Yoshioka, Phys. Rev. C, **97**, 034622 (Mar 2018).
- [34] T. Yamamoto, T. Okudaira, S. Endo, H. Fujioka, K. Hirota, T. Ino, K. Ishizaki, A. Kimura, M. Kitaguchi, J. Koga, S. Makise, Y. Niinomi, T. Oku, K. Sakai, T. Shima, H. M. Shimizu, S. Takada, Y. Tani, H. Yoshikawa, and T. Yoshioka, Phys. Rev. C, **101**, 064624 (Jun 2020).
- [35] T. Yamamoto, T. Okudaira, S. Endo, H. Fujioka, K. Hirota, T. Ino, K. Ishizaki, A. Kimura, M. Kitaguchi, J. Koga, S. Makise, Y. Niinomi, T. Oku, K. Sakai, T. Shima, H. M. Shimizu, S. Takada, Y. Tani, H. Yoshikawa, and T. Yoshioka, Phys. Rev. C, **105**, 039901 (Mar 2022).
- [36] V. V. Flambaum and A. J. Mansour, Phys. Rev. C, **105**, 015501 (Jan 2022).